The use of the high resolution visible in SAFNWC/MSG cloud mask

Marcel Derrien, Herve Le Gleau, Marie-Paule Raoul

THE USE OF THE HIGH RESOLUTION VISIBLE IN SAFNWC/MSG CLOUD MASK

Marcel Derrien, Hervé Le Gléau, Marie-Paule Raoul

METEO-FRANCE, Centre de Météorologie Spatiale, Avenue de Lorraine, BP 50547, Lannion, France

Abstract

NWCSAF (www.nwcsaf.org) consortium continuously develops and maintains a software package to extract various products from Meteosat Second Generation (MSG) imagery. Meteo-France has developed the part of this software package retrieving cloud mask and types, cloud top temperature and height.
The improvement of the detection of small scale low clouds was a challenging task asked by the users of the SAFNWC/MSG cloud mask and type, for an earlier detection of convection and for a better screening of cloud-contaminated pixels prior the use of clear-sky radiances in the study of marine or land surface properties or their assimilation in Numerical Weather Prediction models.
For this aim Meteo-France has developed an algorithm analysing the High Visible Resolution (HRV) of Spinning Enhanced Visible and Infrared Images (SEVIRI) and implemented it as an option in v2010 of the SAFNWC/MSG cloud mask available for users in June 2010.
The paper describes the algorithm based on temporal analysis of HRV features and its application at the coarser spatial resolution of the SEVIRI cloud mask. Real examples illustrate situations where its behaviour can be visually estimated (improvements, misses and false alarms).
Finally, the impact of its implementation is evaluated through a 11 month period by comparison with SYNOP and SHIP ground-based cloud covers. The increase of Cramer's coefficient (a normalized χ^2 indicator) when using HRV denotes that it is better associated with the SYNOP and SHIP ground-based observations of the cloudiness categorized in three classes, clear($N \leq 2$), broken ($3 \leq N \leq 5$) or cloudy ($N \geq 6$).

INTRODUCTION

A better detection of small scale low clouds at daytime was requested by the users of SAFNWC/MSG package during the SAFNWC users workshop held at Madrid in 2005. The advantage of the better spatial resolution of the HRV channel was not exploited by the previous versions of the SAFNWC/MSG cloud detection scheme. Therefore its use was one of the improvement tasks planned during the second phase of the project. The SEVIRI cloud mask algorithm analysed in this paper is an output of this task.

HRV IMAGERY CHARACTERISTICS

SEVIRI has one high resolution (HRes) broadband solar channel (0.3-1.1 μm) and 11 lower resolution (LRes) channels; 3 narrowband solar channels (0.6, 0.8 and 1.6 μm) and 8 thermal infrared channels (3.9, 6.2, 7.3, 8.7, 9.7, 10.8, 12.0 and 13.4 μm). The spectral response functions of the narrowband channels at 0.6, 0.8 μm and HRV channel are shown in figure 1. The HRV sampling increment angle is 251.53/3 μrad in both N/S and E/W direction, in fact 1/3 of LRes bands, leading to a 1x1km2 at sub-satellite point. However, one should note that the true optical resolution is lower by a factor 1.6 for both HRes and LRes (respectively 1.67km and 4.8km at the sub-satellite point, Schmetz et al.,2002). The HRV measurements are performed by 9 detectors, their calibration adjustment, registration between channels, and rectification are performed before the level 1.5 images reach the users through EUMETCast.

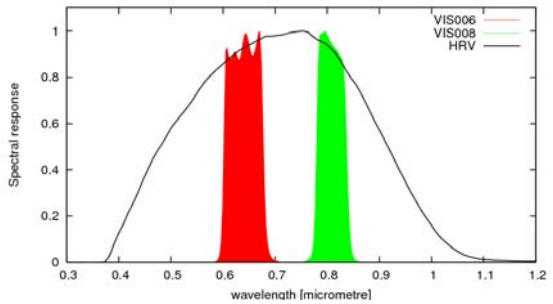

Figure 1: **Spectral response functions of the MSG (Met-9) SEVIRI bands for the 0.6μm band (red) , 0.8 μm (green) and HRV (black).**

A full HRV earth disc would be an image of 11136x11136 points. Due to MSG downlink limitations, only two distinct sub-areas are transferred to the users, the upper zone covering Europe has a fixed position in the disc and the lower one is shifted to follow the daily illumination. Between 00h UTC and 14h UTC, its position is suited to monitor the Indian Ocean, between 14hUTC and 17h UTC it is shifted westwards every hour and between 17h UTC and 00h UTC it remains in a position to monitor the Atlantic Ocean. Figure 2 illustrates the transmission scheme of HRV data. Of course this alternative sectorized coverage is a drawback for the users processing regions not permanently covered by HRV, it is increased by the need of a pair of images for the HRV-based detection algorithm.

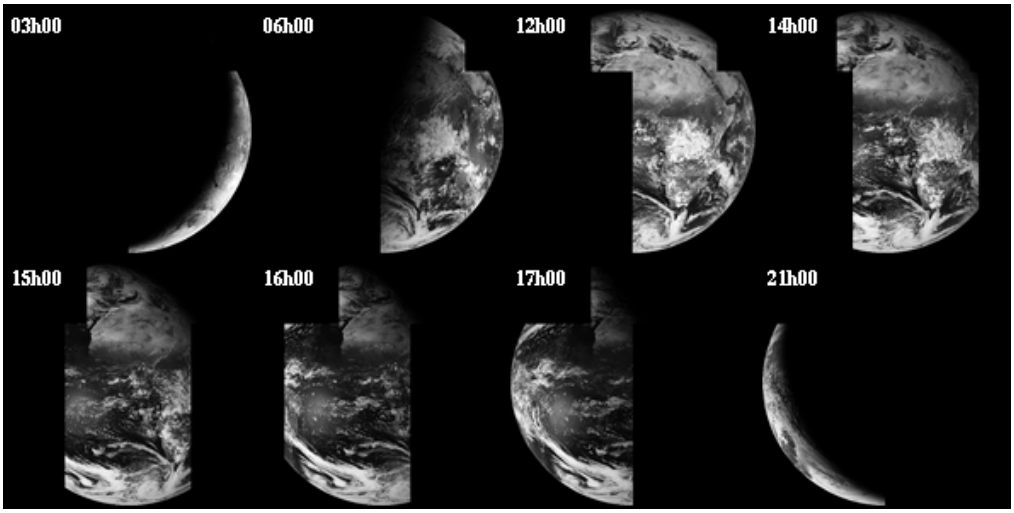

Figure 2: **Illustration of the HRV window positions over MSG earth disc on 14 January 2010.**

The coregistration of images is known by the position of the pixel whose centre corresponds to 0 E resp. 0 N ; in HRV image it is at position (5566,5566) and (1856,1856) in LRes SEVIRI, in the native coordinates (starting at 1 for the lower right pixel of each image). This adjustment is performed by the rectification process. It is an essential prerequisite for a good fusion of HRV and other LRes SEVIRI bands in an instantaneous image and between consecutive images. Deneke and Roebling, 2010 found a minor misregistration of the HRV relative to the narrowband channels of 0.36km±0.11km in East and 0.06±0.10km in South direction for the European area that they have studied. We have neglected this effect in our scheme.

HRV-BASED DETECTION IMPLEMENTATION DETAILS

We designed it as an add-on option of the cloud mask, as some users may be restricted by hardware considerations or would like to avoid changes in cloud detection efficiency for their operational applications. The optional HRV-based algorithm is applied only to SEVIRI pixels remained as clear after the two previous steps of the cloud mask algorithm (SEVIRI spectral and textural thresholding (Derrien and Legleau, 2005) and temporal-differencing and region-growing, (Derrien and Legleau, 2010). It requires not only the HRV data of the current scene, but also the scene observed and analysed 15 minutes sooner.

HRV reflectance test over land

The assumption is that any low cloud exhibits higher HRV reflectance than underlying clear-sky surface. This test is designed to catch static small scale low clouds that are not detected by change detection technique.
A LRes SEVIRI pixel is classified as cloud contaminated if not already classified as cloud by previous tests and if:

- solar elevation > 5° and Max(R_{hrv} 3x3) > R_{hrv}threshold
  Where Max(R_{hrv} 3x3) is the maximum HRV normalized reflectance in the 3x3 HRV array covered by the corresponding SEVIRI LRes pixel.

The threshold is a crude estimate of clear-sky broadband reflectances derived from maps of monthly values and an angular empirical correction. The monthly maps are obtained from a combination of black sky albedo for 3 MODIS narrow bands (0.55μm, 0. 67μm and 0.86μm) available from a NASA website dedicated to MODIS atmosphere (http://modis-atmos.gsfc.nasa.gov/ALBEDO/index.html). Black-sky albedo is the directional hemispherical reflectance computed at local solar noon estimated from MODIS Terra and Aqua measurements.
The parameterization of this test has been designed using a one-year period of collocations of SYNOP and satellite data including HRV. When applied to full disk data during summer 2009 false alarms that were not observed on the training data set and too difficult to remove (not clearly depending on Rmap or scattering angle) appeared in some places. To avoid them, the threshold has been increased lately before the software delivery to the integrator. A consequence is that some rather static topographically induced clouds such as for instance valley fog not directly detected by other SEVIRI visible channels may still remain not detected by this test.

Local spatial HRV texture test over sea

A SEVIRI pixel is classified as cloud contaminated if:

- solar elevation > 10° and [SD(R_{hrv} 3x3)/Mean(R_{hrv} 3x3) > .08 or SD(R_{hrv} 3x3) > 0.8%]
- solar elevation < 10° and solar elevation > 5° and [SD(R_{hrv} 3x3)/Mean(R_{hrv} 3x3) > .16 or SD(R_{hrv} 3x3) > 0.4%]

- Mean(R_{hrv} 3x3) and SD(R_{hrv} 3x3) stand respectively for the mean and standard deviation computed using the 9 reflectances of HRV pixels covered by the SEVIRI low resolution pixel

This test based only on HRV local texture inside SEVIRI low resolution pixel detects heterogeneities over sea, one feature detects small clouds when background is rather dark whereas the other one is more efficient for heterogeneities inside clouds or sunglint, that were not detected by previous test based on other SEVIRI visible channels.

Local spatial texture and temporal test over land

A SEVIRI pixel is classified as cloud contaminated if:

- clear (and not snowy)

and

- [SD(R_{hrv} 3x3) > 5% and MIN(RN_{hrv} 3x3)$_{cur}$ > 10%
  and abs(1.0- MAX_{cur}(RN_{hrv}3x3)/ MAX_{prev}(RN_{hrv}3x3) > 0.03
  and abs(1.0- MIN_{cur}(RN_{hrv}3x3)/ MIN_{prev}(RN_{hrv}3x3) > 0.03]
  or
- [SD(R_{hrv} 3x3) > 1.5% and MIN(RN_{hrv} 3x3)$_{cur}$ > 10%
  and SD_{cur}(R_{hrv} 3x3)/$MEAN_{cur}$(R_{hrv} 3x3) – SD_{prev}(R_{hrv} 3x3)/$MEAN_{prev}$(R_{hrv} 3x3) > 0.03
  and MAX_{cur}(RN_{hrv} 3x3)) > 1.03* MAX_{prev}(RN_{hrv} 3x3))]

-SD MIN MAX MEAN stand respectively for the spatial standard deviation, minimum value, maximum value and mean of the feature.
-R_{hrv} is the HRV reflectance
-RN_{hrv} is the HRV reflectance normalized by the analytical formulation of solar pahthlength valid for a standard atmosphere proposed by Li and Shibata, 2006. (in place of classical inverse cosine function).
-indices $_{cur}$ and $_{prev}$ stands for pixels from the current image or the one 15 minutes sooner.

The assumption behind this test is that a mobile or evolving bright target inside a 3x3 HRV array is a cloud. False alarms that have been problematic are clear sides of cloud shadow limits moving over bright grounds. This is why the pixels detected by this test are further processed by a neighbourhood analysis described below.

Neighbourhood filtering

Clear restoral test over land

This test is designed to remove some false alarms passing through the previous HRV-based tests, and is applied only to pixels detected by this test.
A LRes SEVIRI pixel is restored as clear if:

- Its MEAN(R_{hrv}3x3) is minimum among other land pixels in its SEV_{3x3} low resolution neighbourhood

Cloud restoral test over land

Obviously during visual inspection of the results some clouds remained missed after the change detection test. Brighter pixels in the neighbourhood of pixels detected as clouds by the HRV change detection algorithm described in the previous sections should also be detected as cloudy. This test is designed to this purpose.
A SEVIRI pixel on land at low resolution scale in the 11x11 neighbourhood of a HRV change detection is restored as cloud if at least 5 pixels inside 11x11 neighbourhood are detected by HRV change detection tests and if:

- $MIN(RN_{hrv}\,3x3)_{cur} > 10\%$

and

- $MAX(R_{hrv}\,3x3) > MEAN_{11x11}(Max(R_{hrv}\,3x3)$ of the pixels detected by HRV if nb > 5)

and

- $SD(R_{hrv}\,3x3) > 1.5\%$

  or

  $MAX(R_{hrv}\,3x3)-MIN(R_{hrv}\,3x3) >$
  $MEAN_{11x11}(MAX(R_{hrv}\,3x3)- MIN(R_{hrv}\,3x3))$ of the pixels detected by HRV if nb > 5)

EXAMPLES OF HRV-BASED ALGORITHM IMPACT

We have analysed the spatial and temporal distribution of HRV-based detections by counting their occurrences on a monthly base. Figure 3 illustrates its impact on derived full disc cloud observation frequency.

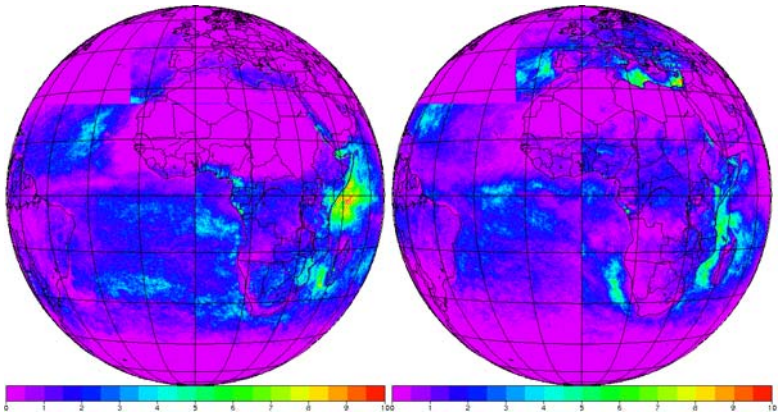

Figure 3: **HRV-based detection frequency for January 2010 (left) and July 2010 (right)**

Maritime cloud patterns

Two rather difficult cloud patterns are illustrated. The figures show how HRV resolves the cloud field when compared with the low resolution SEVIRI visible band and how the HRV-based detections are transposed at the SEVIRI LRes through the Cloud Type. One can also note that generally these detections correspond to either fractional or low clouds in the CT cloud type product.

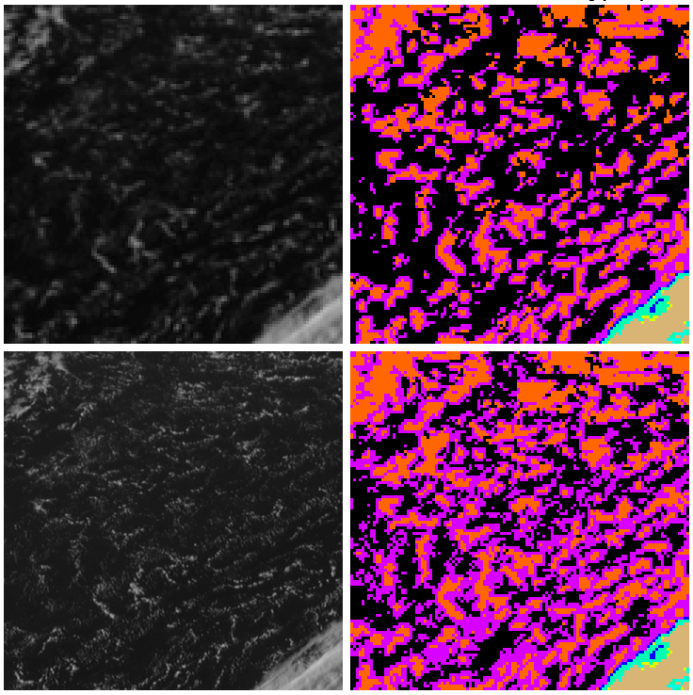

Figure 4: **Shallow convection clouds over Northern Atlantic, 8 September 2009. 17h00UTC, (120x120 LRes size). Top left: 0.8 μm reflectance; top right: v2009 cloud type; bottom left: HRV reflectance; bottom right: v2010 cloud type**

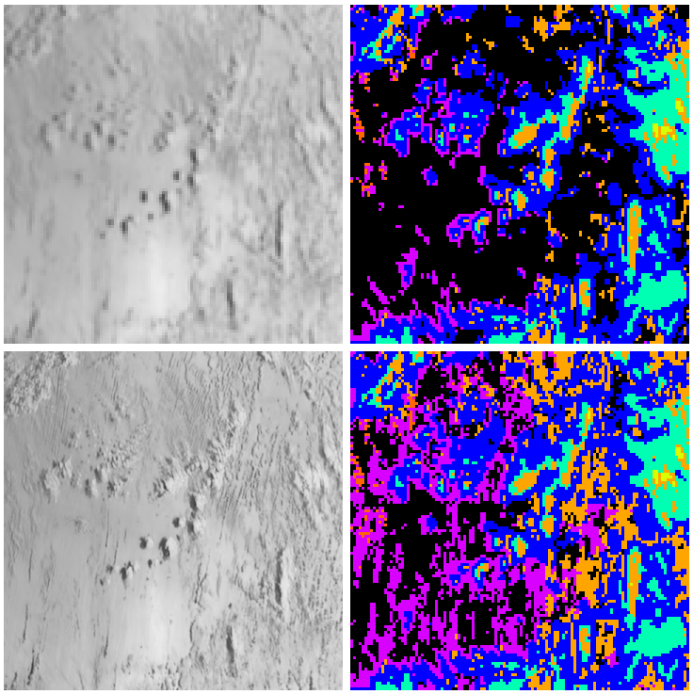

Figure 5: **Sunglint with trade-wind convective low clouds over Indian Ocean, 8 September 2009, 04h00UTC, (120x120 at low resolution SEVIRI scale). Top left: 0.8 μm reflectance; top right: v2009 cloud type; bottom left: HRV reflectance; bottom right: v2010 cloud type**

Continental cloud patterns

Two cases are used to illustrate a typical fair-weather convection over a desertic area in Africa (figure 6) and over Europe (figure 7).

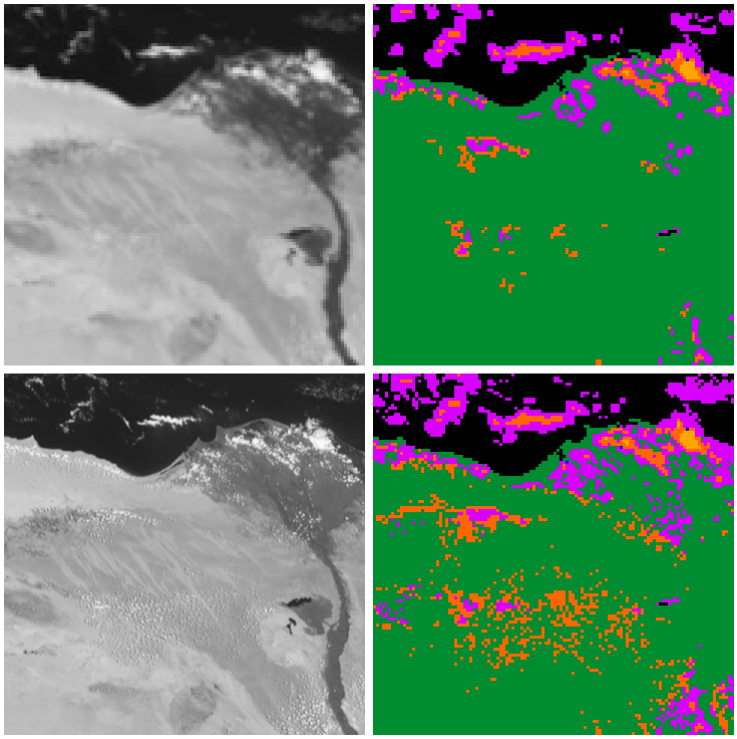

Figure 6: **Fair-weather cumulus over Egypt near Nile delta, 9 September 2009, 10h00UTC, (120x120 LRes size). Top left: 0.6 μm visible reflectance; top right: v2009 cloud type; bottom left: HRV reflectance; bottom right: v2010 cloud type.**

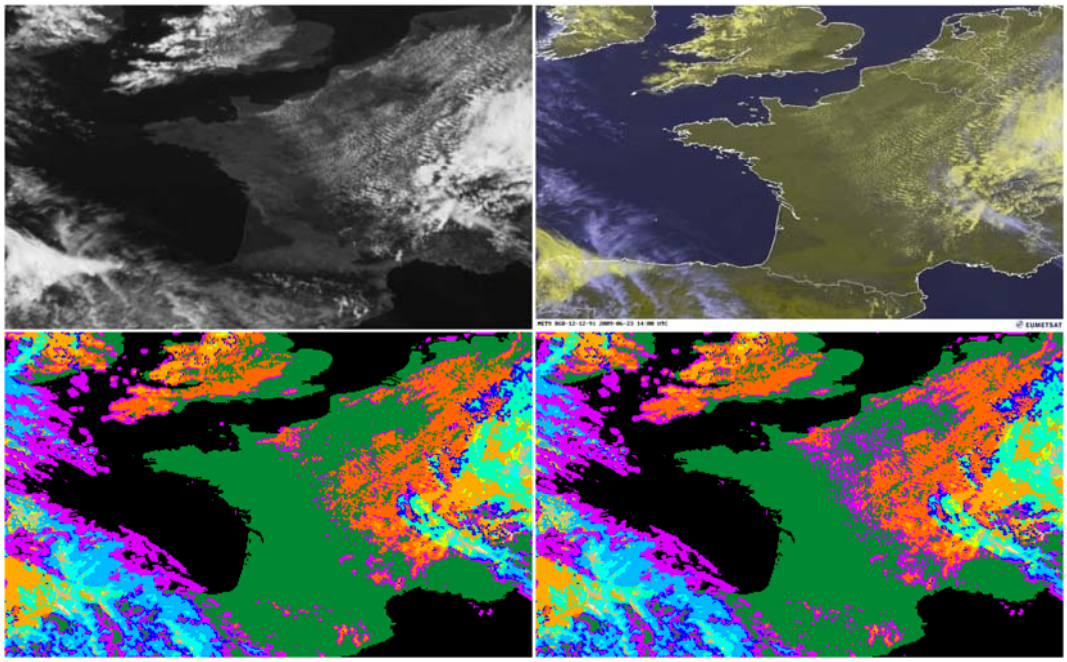

Figure 7: **Fair-weather cumulus in subsident air over western Europe, 23 June 2009, 14h00UTC, (1270x770 LRes size). Top left: enhanced 0.6 μm visible reflectance; top right: EUMETSAT RGB (12-12-9); bottom left: v2009 cloud type; bottom right: v2010 cloud type.**

FULL EARTH DISC AND SYNOP AND SHIP CLOUD COVERS COMPARISON

We have specifically studied the HRV-based cloud detections using SYNOP over land, provided by M.Lockhoff from CM-SAF, and SHIP over sea, for the available eleven-month period (from October 2009 to August 2010). As those detections are sensitive to fractional cloudiness, the method as described in Derrien and Legleau,2005 used to assess the cloud detection accuracy of cloudy and clear events, is no longer appropriate to estimate the improvement using HRV data, as it ignores the partial cloud covers.

We have categorized cloud cover in three classes to account for every cloudiness: clear when N≤2, broken when N=3,4,5, cloudy when N≥6. Satellite-based cloud cover is determined by counting any CMa cloud contaminated pixel in the 5x5 SEVIRI LRes box centred on the ground measurement position as 100% covered. Obviously this assumption is not always true particularly for situations when the HRV is likely to detect a cloud while the coarser SEVIRI missed it. Therefore we can note that the satellite-based cloud cover is by definition biased towards the cloudy class. Three-by-three confusion matrices are built, and the resulting classifications scheme are studied. The population is restricted to cases where at least one LRes pixel in 5x5 box is detected by HRV test and where satellite zenith angle is lower than 78 degrees. For this population the two satellite-based cloud covers (noted v2010,with HRV and v2009, without HRV) are determined, their confusion matrices are given in tables 1 and 2. We note that broken ground-based cloudiness is 50% of the population when HRV test triggers at least once inside the 5x5 box (16% when all SYNOP of the period are considered). We note also our satellite-based classification trend to overestimate ground-based cloudiness, but our method counts every cloud detection as 100% covered by clouds.

	Cloud Mask Cloudy	**Cloud Mask Broken**	**Cloud Mask Clear**	**Total**
Observed Cloudy	39718 (24961)	16394 (24297)	4310 (11164)	60422
Observed Broken	62772 (31356)	50071 (56424)	20626 (45689)	133469
Observed Clear	16941 (7694)	26675 (21383)	28966 (43505)	72582
Total	119431 (64011)	93140 (102104)	53902 (100358)	266473

Table 1: Confusion matrices for cloud mask v2010 and (v2.009) cloud covers at daytime for every SYNOP in the MSG earth disc from 1 October 2009 to 31 August 2010 when any HRV detection occurred in the 5x5 satellite target and with satellite zenith angle <78°

	Cloud Mask Cloudy	**Cloud Mask Broken**	**Cloud Mask Clear**	**Total**
Observed Cloudy	995 (586)	352 (509)	168 (420)	1515
Observed Broken	2874 (1378)	1725 (1825)	992 (2388)	5591
Observed Clear	750 (294)	878 (673)	847 (1508)	2475
Total	4619 (2258)	2955 (3007)	2007 (4316)	9581

Table 2: Confusion matrices for cloud mask v2010 and (v2009) cloud covers at daytime for every SHIP in the MSG earth disc from 1 October 2009 to 31 August 2010 when any HRV detection occurred in the 5x5 satellite target and with satellite zenith angle <78°

The Cramer's coefficient, that is in fact a normalization of the chi-square test to the data set size and the confusion matrix size, presents the advantage that its range lies between 0 (no correlation) and 1 (perfect correlation). It is defined as :

$$V = \sqrt{\frac{\chi 2}{NxMIN(r,c)}}$$

Where N is the total number of events of the confusion matrix, r and c are the numbers of rows and columns of the confusion matrix and χ^2 is the chi-square test. The table 3 shows that it increases when the satellite-based cloudiness includes the HRV detections.

	V2009	V2010
Land	0.24099	0.257772
Sea	0.170707	0.180439

Table 3: **Cramer's coefficients for v2009 and v2010 cloud cover classifications in three classes (cloudy,broken,clear) stratified by background for the subset where HRV detection triggers at least once in the 5x5 satellite target and with satellite zenith angle <78°**

CONCLUSION

The SAFNWC/MSG v2010 cloud mask at low SEVIRI resolution makes use of HRV information to better account for partial cloudiness inside SEVIRI pixels. The complementary HRV detection algorithm, applied only on pixels not flagged as cloudy by the primary cloud mask, exploits spectral, textural and temporal HRV features. By comparison with SYNOP and SHIP ground-based cloud covers over the full earth disc we have assessed an improvement when considering a three-class categorization of cloudiness (clear, broken, cloudy), of course this improvement depends on the efficiency of the initial cloud mask used in the comparison.
We have also visually inspected resulting cloud masks, few observed false alarms are cloud shadows over bright backgrounds and misses may still occur over static orographic loud clouds. The quality of SAFNWC/MSG cloud mask over the lower part of the earth disc depends on the presence the HRV data in the pair of images required by the method. Therefore SAFNWC/MSG users processing such regions may decide to use it or not when configuring their applications, moreover HRV effective use is reported at the pixel level in the cloud mask quality information.
The fusion of high and low resolution imagery is a challenging task of future geostationary meteorological satellites, such as Meteosat Third Generation. In the context of cloud detection, as a feedback of this work, we think that cloud shadows and terrain orientation effects in visible imagery will require a particular attention with the advances in spatial resolution.

REFERENCES

Deneke, H.M. and Roebling, R., (2010) Downscaling of METEOSAT SEVIRI 0.6 and 0.8 micron channel radiances utilizing the high-resolution visible channel, *Atmos. Chem. Phys. Discuss.*, **10**, pp 10707-10740

Derrien, M., and Le Gléau, H., (2005) MSG/SEVIRI Cloud Mask and Type from SAFNWC, *International Journal of Remote Sensing* ,**21**, pp 4707–4732, DOI: 10.1080/01431160500166128

Derrien, M., and Le Gléau, H.,(2010) Improvement of cloud detection near sunrise and sunset by temporal-differencing and region-growing techniques with real-time SEVIRI, *International Journal of Remote Sensing* , **31**, 7, pp 1765–1780 DOI: 10.1080/01431160902926632

Li, J. and Shibata, K., (2006) On the effective solar pathlength, *Journal of the Atmospheric Science*, **63**, 4, pp 1365-1373

Schmetz, J., Pili, P., Tjemkes, S., Just, D., Kerkmann, J., Rota, S., and Ratier, A., (2002) An introduction to Meteosat Second Generation (MSG), *B. Am. Meteorol. Soc*., **83**, pp 977–992